Vol. 47 (2016) ACTA PHYSICA POLONICA B No 3

STUDIES OF PREDICTIVE POWERS OF BETA-DELAYED NEUTRON EMISSION MODEL BASED ON EFFECTIVE DENSITY PARAMETRIZATION*

Krzysztof Miernik

University of Warsaw, Faculty of Physics, Warszawa 02-093, Poland

(Received December 18, 2015)

Effective density model of beta-delayed neutron emission is studied for its predictive powers. The parameters of the model are fitted to the reduced experimental dataset in order to check for a short-range extrapolation accuracy. Different mass models are used for a study of a long-range extrapolations.

DOI:10.5506/APhysPolB.47.739

1. Introduction

Beta-delayed neutron emission (βn) is a decay mode opened in neutron-rich nuclides whenever beta-decay energy (Q_β) is larger than decay daughter neutron separation energy (S_n). The importance of this decay mode is growing with the excess of neutrons and, eventually, it becomes a dominant decay mode for the most currently known exotic neutron-rich isotopes. Delayed neutrons play an important role in operation of nuclear reactors as well as in astrophysical models of the r-process [1].

Theoretical mass models predict about 8000 nuclides to be bound. More than a half of these meet energy conditions for β-delayed neutron emission. The current experimental knowledge is limited to less than 200 measured total delayed neutron emission probabilities (P_n). Most of the information on that process relevant for the r-process modeling is missing, mainly due to difficulties in production of very neutron-rich isotopes. It is obvious that theoretical models of delayed neutron emission are needed. One of such models, focused on calculating P_n values, is a phenomenological model based on effective density parametrization [2]. The P_n (defined as probability of

* Presented at the XXXIV Mazurian Lakes Conference on Physics, Piaski, Poland, September 6–13, 2015.

emission of one or more neutrons) for a given nuclide can be calculated with a following formula

$$P_n = \frac{\int_{S_n}^{Q_\beta} S_\beta(E) f(Z+1, Q_\beta - E) dE}{\int_0^{Q_\beta} S_\beta(E) f(Z+1, Q_\beta - E) dE}\,, \tag{1}$$

where E is the excitation energy of the daughter nuclide, S_β is the β-strength function (*cf.* Eq. (2)), f is the Fermi integral.

In order to calculate the βn emission probability, a knowledge of the β-strength function (S_β), which holds the nuclear structure description, is crucial. The effective density model is based on assumption that S_β is proportional to the total level density

$$S_\beta(E) \sim \rho(E) = \frac{\exp\left(a_d\sqrt{E}\right)}{E^{3/2}}\,. \tag{2}$$

Since not all of the states can participate in β-decay, the a_d here is an effective parameter and, in general, does not describe a realistic level density. The systematics of the a_d were based on experimental P_n values for 163 nuclides and modeled with a phenomenological function [2].

Thus, the parametrization of a_d allows for calculations of P_n for a whole chart of nuclides with use of some mass model needed to find the Q_β and S_n values. The predictive powers of this approach are studied in this contribution. More details concerning the model are given in Refs. [2–4].

2. Short-range extrapolations

In order to study the dependency of the model predictions on different mass models, the experimental data for $Z < 8$ were discarded leaving a dataset of 155 entries. From this group, a subset of 114 points was created by removal of the most neutron-rich isotopes for each element (if at least one data point was present). The parameters were refitted to this reduced set, and subsequently predictions for 41 previously removed nuclides (these are: ^{24}O, ^{25}F, ^{28}Ne, ^{34}Na, ^{35}Mg, ^{35}Al, ^{37}Si, ^{42}P, ^{44}S, ^{46}Cl, ^{50}Ar, ^{53}K, ^{63}V, ^{65}Mn, ^{72}Co, ^{77}Ni, ^{79}Cu, ^{81}Zn, ^{84}Ge, ^{85}Ga, ^{87}As, ^{91}Se, ^{94}Br, ^{99}Kr, ^{102}Rb, ^{102}Sr, ^{103}Y, ^{110}Nb, ^{113}Tc, ^{119}Rh, ^{123}Ag, ^{132}Cd, ^{134}In, ^{136}Sn, ^{139}Sb, ^{138}Te, ^{140}I, ^{145}Xe, ^{148}Cs, ^{149}Ba, and ^{150}La) were studied. The predictive powers are measured by a normalized $\chi^2_{\rm n}$ function (χ^2 divided by number of points).

A summary of calculations is presented in Table I, where $\chi^2_{\rm n}$ was calculated with full and reduced parametrization for both full dataset and the most neutron-rich subset. The results show that the model is capable of a short-range extrapolation, and the subset of most neutron-rich nuclides is not the most contributing factor to the overall χ^2_{n}. The parametrization obtained from a reduced dataset is practically equally well describing both the whole dataset and the removed points.

TABLE I

Normalized χ^2_{n} values for parametrization obtained with full and reduced data-set calculated over full dataset and for subset of most neutron-rich nuclides. See the text for more details.

	Dataset	
Parametrization	Full (155)	Subset (41)
Full (155)	67	22
Reduced (114)	71	28

The P_n values calculated with Eq. (1) are sensitive to the Q_β and S_n values. The AME-12 mass tables [5] used for the parametrization of the model include some extrapolated masses. The subset of 41 most neutron-rich isotopes includes 19 extrapolated values (in all cases both Q_β and S_n). The calculations were performed with 4 different mass models (FRDM-95 [6], HFB-24 [7], KTUY-05 [8], and DZ-96 [9, 10]) for the subset of 41 nuclides, and the normalized χ^2_{n} was calculated. The results are summarized in Table II. Since the χ^2 are of the similar order or smaller, then the results obtained with the experimental data (AME-12) in all the cases, one can deduce that the main contribution to the discrepancies are the deficiencies of the model not those of the mass models. Consequently, the short-range extrapolations should not be significantly affected by the chosen mass model. Figure 1 presents comparison of predictions of different mass models compared to the experimental data. The pattern is clearly preserved in all cases, regardless of the used model.

TABLE II

Normalized χ^2_{n} values for the 41 most neutron-rich nuclides subset calculated with different mass models used. See the text for more details.

Mass model	χ^2_{n}
AME-12	28
FRDM	30
HFB-24	23
KTUY-05	16
DZ-96	20

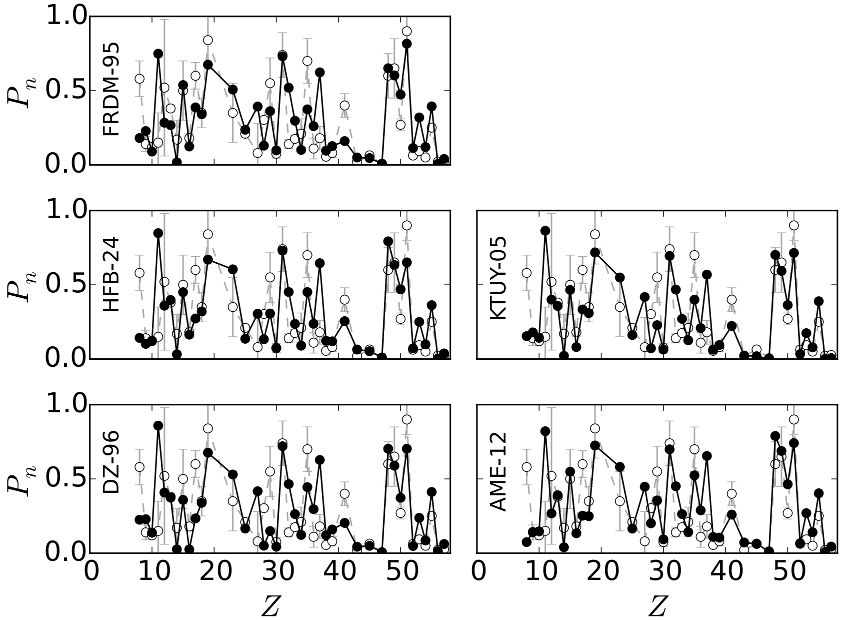

Fig. 1. Comparison of P_n values calculated with use of different mass models (black symbols, solid line) with experimental values (open symbols, dashed line) for subset of 41 most neutron-rich nuclides. See the text for more details.

2.1. Long-range extrapolation

Extrapolations in the area where no experimental data are available can be only studied by means of use of different mass models. For delayed neutrons emission, the energy window $Q_{\beta n} = Q_\beta - S_n$ is more important than absolute mass values, so this parameter was used for comparison of mass models. It is worth noticing that even though the discrepancies of models for known nuclides are of similar order with Root Mean Square (RMS) of $Q_{\beta n}$ of about 0.6 MeV, the predictions for the unknown isotopes can vary significantly (with RMS between models from 0.8 to 1.5 MeV). This is shown in Fig. 2, where difference between calculated and experimental $Q_{\beta n}$ is shown in black, and difference between given model and HFB-24 (yielding lowest RMS compared to experimental data of 0.55 MeV) in gray.

The results of calculations of effective density model with different mass models were studied by means of parameters

$$A^i_{km} = \frac{P^k_n(i) - P^m_n(i)}{P^k_n(i) + P^m_n(i)}\,, \tag{3}$$

$$A'^i_{km} = \frac{\left|P^k_n(i) - P^m_n(i)\right|}{P^k_n(i) + P^m_n(i)}\,, \tag{4}$$

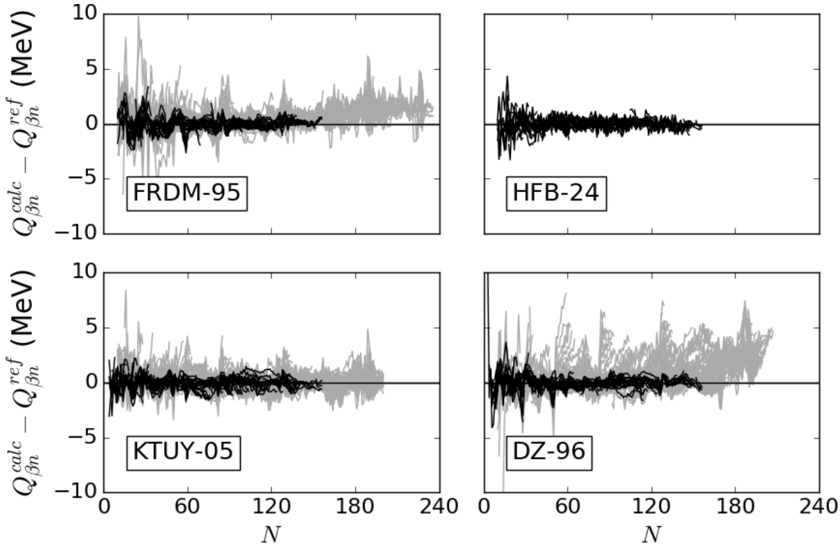

Fig. 2. $Q_{\beta n}$ values calculated by theoretical models compared to experimental values (black) and to HFB-24 mass model (gray).

where index i denotes selected nuclide, k and m — selected models. The parameters constructed as a sum for all common nuclei show average relative deviation between models (A'_{km}) and trend of deviation (A_{km}).

The region of delayed neutron emission is presented in Fig. 3, where HFB-24 mass model was used to calculate size of delayed neutron emission window $Q_{\beta n}$ relative to the total decay energy Q_β. The whole mass surface was divided into three areas defined by N/Z ratio (I: 1.3–1.7, II: 1.7–1.9, and III: 1.9–3.0). The first region includes area with the highest number of experimentally known cases, and is on the boundary of fulfilling emission conditions. The second region includes the isotopes of the r-process path [11], and the third the most neutron-rich nuclides up to the limit of spontaneous neutron emission.

In the region III, the $Q_{\beta n}$ in most of the cases is large enough that almost 100% decays are followed by the delayed neutron regardless of the used model. The region I, on the contrary, is very sensitive to the small differences in predicted masses since many isotopes are on the limit of delayed neutron emission. The region II is characterized by moderate P_n values, most of the data points from subset of 41 isotopes is located in that region (*cf.* Fig. 3). The results of calculations are summarized in Fig. 4, where the A^i parameter is presented for all pairs of models.

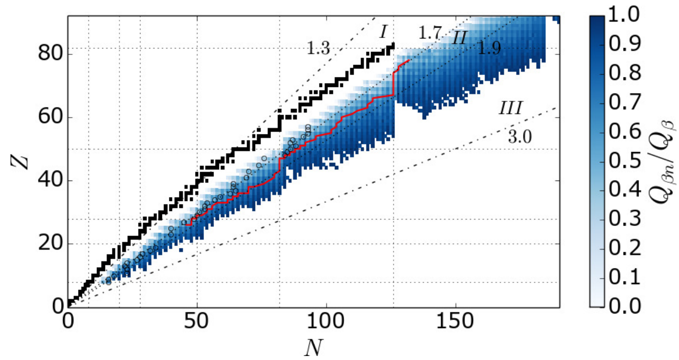

Fig. 3. (Color on-line) Energy window for delayed neutron emission relative to the total decay energy calculated with HFB-24 mass model. The regions defined by N/Z ratio are shown by dotted lines. The solid (red) line shows the approximate r-process path. The circles show location of the 41 isotopes removed in short-range extrapolation tests.

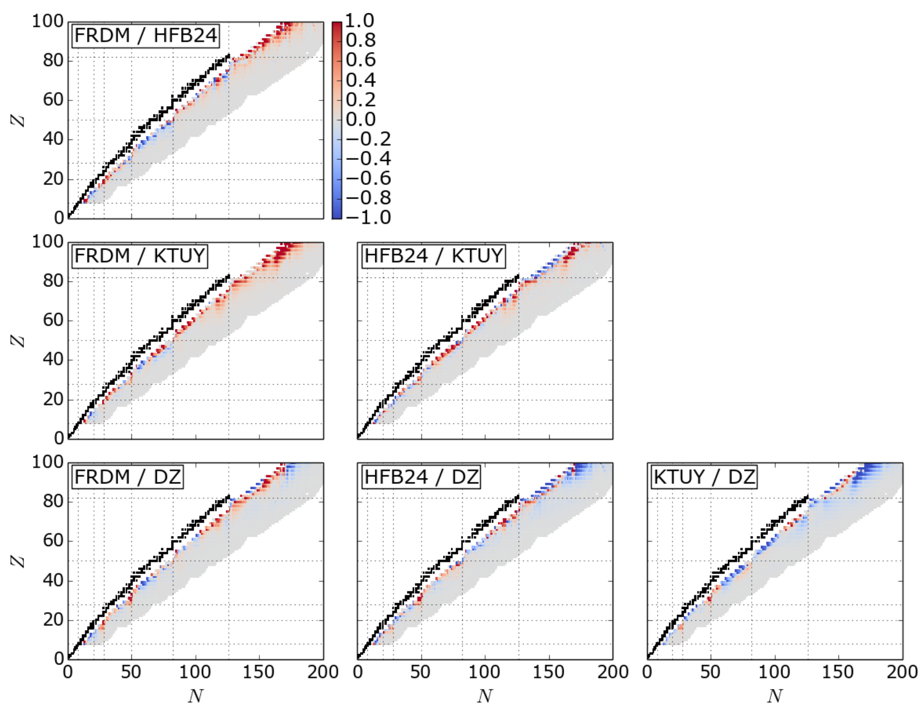

Fig. 4. (Color on-line) Charts of nuclides showing parameter A^i values calculated for all pairs of mass models. The results are color-coded according to the scale shown next to the first plot.

The A and A' parameters (sum for all nuclides) calculated for all pairs of models for the region II (around r-process path) are shown in Table III. Typical deviation between models is at the level of 20%, and it should be considered as uncertainty of the result of calculations due to mass-models uncertainties. At the same time, the A' values calculated for the 41 most neutron-rich isotopes between experimental results and calculated ones yielded 25–30%. Therefore, the impact of the uncertainty of mass models in region II should be considered of similar order as the uncertainty of the model itself (20%). Another important observation refers to the systematic deviations between models. It is clearly seen in Fig. 4 and in Table III that some models have systematic tendencies compared to other models. The predictions based on FRDM model are on average giving larger P_n values than any other mass model. Those based on KTUY model are, on the contrary, the smallest. There are also similarities between the models: the KTUY results are close to those of the HFB models, and DZ to FRDM. As expected, these similarities have reflection in low RMS for $Q_{\beta n}$ calculated over whole mass surface between these pairs of models, HFB–KTUY yielding 0.8 MeV and FRDM–DZ 1.0 MeV. It is interesting to notice that FRDM and KTUY are, in general, macroscopic–microscopic models, while HFB and DZ are purely microscopic. Apparently, the differences are not due to the method of calculations but rather to uncertainties of extrapolation of model parameters outside the known area.

TABLE III

A and A' (in brackets) values calculated between predictions of P_n values in region II based on different mass models. See the text for more details.

	FRDM-95	HFB-24	KTUY-05	DZ-96
FRDM-95	—	0.158 (0.233)	0.218 (0.256)	0.055 (0.184)
HFB-24	−0.158 (0.233)	—	0.074 (0.207)	−0.099 (0.234)
KTUY-05	−0.218 (0.256)	−0.074 (0.207)	—	−0.152 (0.226)
DZ-96	−0.055 (0.184)	0.099 (0.234)	0.152 (0.226)	—

3. Summary

The effective density model of delayed neutron emission was tested for its predictive powers. It was shown that the short-range extrapolations (1–3 neutrons away from the known area) should be possible with deviations on the similar level as the description of the dataset used for parametrization. The average relative uncertainty of the model is at the level of 20%. The long-range extrapolations into generally unknown area may be affected by significantly different predictions of masses by available mass models. The impact of the uncertainties of masses is of similar order as the one introduced by the emission model. It is worth noticing that only the total neutron emission probability (of one or more neutrons) was studied. In the region of r-process path, a two- and three-delayed neutron emission process is predicted to take place [3], and the uncertainties for that type of decay are much larger due to very limited experimental data and lack of possibilities of comparison of theoretical models to measurements. In future, when appropriate data are available, a similar study of the multi-neutron emission should be carried out in order to estimate the uncertainty of predictions of these processes.

REFERENCES

[1] D. Abriola *et al.*, IAEA Report INDC(NDS)0599 (2011).
[2] K. Miernik, *Phys. Rev. C* **88**, 041301(R) (2013).
[3] K. Miernik, *Phys. Rev. C* **90**, 054306 (2014).
[4] K. Miernik, *Acta Phys. Pol. B* **46**, 717 (2015).
[5] G. Audi *et al.*, *Chin. Phys. C* **36**, 1157 (2012).
[6] P. Moller *et al.*, *At. Data Nucl. Data Tables* **59**, 185 (1995).
[7] S. Goriely, N. Chamel, J.M. Pearson, *Phys. Rev. C* **88**, 024308 (2013).
[8] H. Koura *et al.*, *Prog. Theor. Phys.* **113**, 305 (2005).
[9] J. Duflo, A. Zuker, *Phys. Rev. C* **52**, R23 (1995).
[10] J. Duflo, A. Zuker, private communication to AMDC (10 parameters formula), 1996.
[11] K.-L. Kratz, *Astrophys. J.* **403**, 216 (1993).